

On the origin of nitrogen-induced retardation of boron diffusion in amorphous silica

Chin-Lung Kuo and Gyeong S. Hwang^{a)}

Department of Chemical Engineering, University of Texas, Austin, Texas 78713, USA

(Received 9 January 2008; accepted 16 January 2008; published online 6 March 2008)

The effect of N incorporation on B diffusion in amorphous SiO₂ is presented based on spin-polarized density functional theory calculations. Our results show that N incorporation leads to the decrease of O vacancy concentration, which is largely responsible for the retarded B diffusion by reducing diffusion mediators such as *E'* and *S* centers. We also determine the ground state structure of the B—N complex, along with possible formation routes. The direct B—N bonding interaction appears to only slightly increase the activation energy of B diffusion. © 2008 American Institute of Physics. [DOI: 10.1063/1.2840698]

Continued scaling of metal-oxide-semiconductor devices has raised concerns regarding diffusion of dopants and defects in an ultrathin SiO₂ layer which is widely used as the gate dielectric layer. In particular, boron penetration from the heavily *p*-doped polysilicon gate electrode through the thin SiO₂ layer to the Si substrate has been a major concern, relevant to not only gate dielectric quality but also device operation.

It is now well known that B diffusion is suppressed by N incorporation in the oxide layer. Several mechanisms have been proposed to explain the effect of N incorporation on B diffusion in SiO₂. Included are (i) changes in the SiO₂ bonding structure, which may mechanically hinder B diffusion,¹ (ii) reduction of peroxy linkage (Si—O—O—Si) defects by ≡Si—O—N—O—Si≡ formation, as they are thought to mediate B diffusion,² (iii) reduced availability of H by N—H bonding while H is known to enhance B diffusion,³ and (iv) reduced diffusivity of SiO molecules which are generated at the Si/SiO₂ interface and tend to enhance B diffusion.⁴ The existing explanations may appear plausible but they do not provide atomistic details of the correlation between B diffusion and N incorporation in SiO₂.

In this letter, we present the influence of N on B diffusion in *a*-SiO₂ based on combined Metropolis Monte Carlo and gradient corrected density functional theory calculations. We determine the atomic geometries and diffusion pathways of B atoms and also look at how N incorporation affects B diffusion in *a*-SiO₂. Knowing that B diffusion is significantly suppressed even with a small amount of N (~2 at. %),⁵ our primary focus is on addressing the underlying causes of B diffusion retardation in the absence of direct B—N bonding interaction. In addition, we examine possible B trapping by N atoms and its effect on B diffusion. The improved understanding will provide valuable hints as to effective suppression of B penetration as well as precise control of gate oxide nitridation.

We first prepared three *a*-SiO₂ supercells which contain 25 or 33 SiO₂ units within the continuous random network (CRN) model with fourfold-coordinated Si and twofold-coordinated O. Starting with randomly distributed Si and O atoms in a given supercell with a fixed experimental density

of 2.2 g/cm³, the SiO₂ system was relaxed via a sequence of bond transpositions using the Metropolis Monte Carlo (MMC) sampling method based on Keating-like interatomic potentials.⁶ The *a*-SiO₂ structures were further relaxed using density functional calculations (as detailed below). The CRN-MMC approach has been used to construct *a*-SiO₂ structures.^{6–9}

All atomic structures and energies reported herein were calculated using a planewave-basis set pseudopotential method within the generalized gradient approximation of Perdew and Wang (GGA-PW91) (Ref. 10) to spin-polarized density functional theory, as implemented in the well-established Vienna *ab initio* simulation package (VASP).¹¹ Vanderbilt-type ultrasoft pseudopotentials were used for core-electron interactions. A planewave cutoff energy of 300 eV was used. The convergence of atomic configurations and relative energies with respect to plane-wave cutoff energy was carefully checked. The Brillouin zone sampling was performed using a Monkhorst–Pack (2 × 2 × 2) mesh of *k* points, sufficient for the disordered SiO₂ structures considered in this work. All atoms were relaxed using the conjugate gradient method until residual forces on constituent atoms become smaller than 5 × 10^{−2} eV/Å. Diffusion pathways and barriers under the static approximation were estimated using the nudged elastic band method, which allows systematic search for a minimum energy path between two local minima with no prior knowledge about a potential energy surface.

We begin by discussing the structure and diffusion of B in defect-free *a*-SiO₂. Figure 1 (upper panel) shows the minimum-energy structures of B-related defects in *a*-SiO₂. In the neutral state, the threefold-coordinated =B—Si= structure [where — and · represent a Si—O bond and a dangling bond, respectively, see Fig. 1(a)] is predicted to be 0.8 ± 0.6 eV more favorable than the nearly degenerate twofold-coordinated ≡Si—B— [Fig. 1(d)] and boron-oxygen hole center \dot{O} —B(Si≡)₂ [Fig. 1(e)]. We also find that the =B—Si= state [Fig. 1(a)] can convert to the =B—Si≡ [Fig. 1(b)] or the =B— state [Fig. 1(c)] while liberating an *E'* center \dot{Si} ≡ [Fig. 1(h)] or an *S* center = \dot{Si} —Si≡ [Fig. 1(f)], respectively, i.e., =B—Si= → =B—Si≡ + \dot{Si} ≡ or =B—Si= → =B— + = \dot{Si} —Si≡. The transformation reactions appear to occur

^{a)} Author to whom correspondence should be addressed. Electronic mail: gshwang@che.utexas.edu

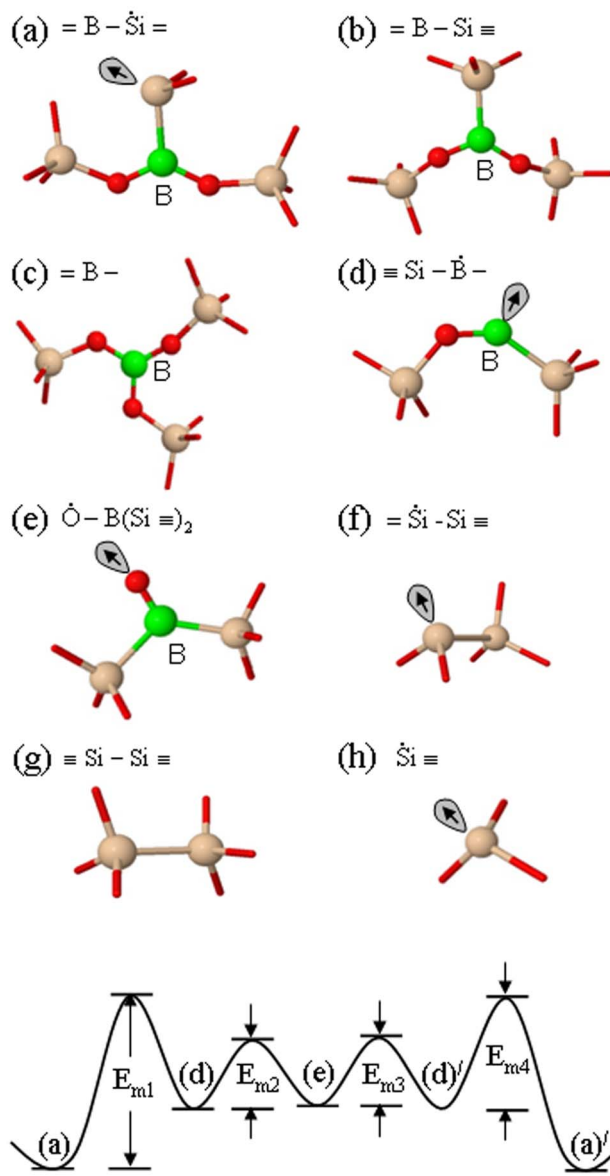


FIG. 1. (Color online) The atomic configurations of B-related defects in a -SiO₂ (upper panels). The small dark (red), big gray (pink), and light (green) balls indicate O, Si, and B atoms, respectively. The locations of unpaired electrons are also indicated. The lower panel shows a viable pathway of B diffusion in a -SiO₂, starting from the $\equiv\text{B}-\dot{\text{S}}\text{i}=\text{}$ state.

with no noticeable energy gain or loss. An S defect center may further dissociate into an O vacancy and an E' center, i.e., $\equiv\dot{\text{S}}\text{i}-\text{Si}\equiv \rightarrow \equiv\text{Si}-\text{Si}\equiv + \dot{\text{S}}\text{i}\equiv$, which turns out to be endothermic by approximately 0.2 eV. In addition, we can expect that combination of two E' centers will result in an O vacancy, i.e., $\equiv\dot{\text{S}}\text{i} + \dot{\text{S}}\text{i}\equiv \rightarrow \equiv\text{Si}-\text{Si}\equiv$, which is predicted to be exothermic by 3.4 eV from our cluster model calculation [with (HO)₃Si—Si(OH)₃]. To achieve good statistics, here we checked the relative stability of the B and defect structures at more than ten different locations in the three a -SiO₂ supercells considered.

As illustrated in Fig. 1 (lower panel), the neutral $\equiv\text{B}-\dot{\text{S}}\text{i}=\text{}$ complex can undergo diffusion which involves a series of reconfiguration processes, i.e., $\equiv\text{B}-\dot{\text{S}}\text{i}=\text{}$ $\xrightarrow{E_{m1}}$ $\equiv\text{Si}-\dot{\text{B}}-\text{}$ $\xrightarrow{E_{m2}}$ $\text{O}-\text{B}(\text{Si}\equiv)_2$ $\xrightarrow{E_{m3}}$ $\equiv\text{Si}-\dot{\text{B}}-\text{}$ $\xrightarrow{E_{m4}}$ $\equiv\text{B}-\dot{\text{S}}\text{i}=\text{}$. The corre-

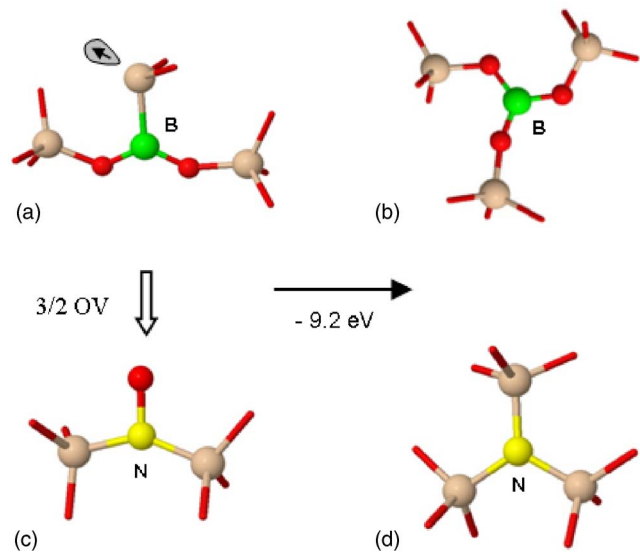


FIG. 2. (Color online) Schematic illustration of the role of N as a scavenger for O vacancies created by B in a -SiO₂. In defect-free a -SiO₂, the $\equiv\text{B}-\dot{\text{S}}\text{i}=\text{}$ and $\text{O}-\text{N}(\text{Si}\equiv)_2$ states may convert to the $\equiv\text{B}-\text{}$ and $\text{N}(\text{Si}\equiv)_3$ states through the transfer of O vacancies. The resulting energy gain is predicted to be 9.2 eV. The small dark (red), big gray (pink), and light (green) balls indicate O, Si, and B atoms, respectively. The locations of unpaired electrons are also indicated.

sponding energy costs are predicted to be $E_{m1} = 2.1 \pm 0.5$ eV, $E_{m2} = 0.7 \pm 0.1$ eV, $E_{m3} = 0.7 \pm 0.1$ eV, and $E_{m4} = 1.2 \pm 0.5$ eV, respectively. On the other hand, the $\equiv\text{B}-\text{Si}\equiv$ and $\equiv\text{B}-\text{}$ states appear immobile due to large activation energies required for breaking strong B—O bonds. However, they may convert to the mobile $\equiv\text{B}-\dot{\text{S}}\text{i}=\text{}$ complex by capturing mobile E' and S centers (which are predicted to undergo migration by overcoming barriers of < 1.3 eV and 1.5 ± 0.6 eV, respectively). The energy costs for the combination reactions $\equiv\text{B}-\text{Si}\equiv + \dot{\text{S}}\text{i}\equiv$ and $\equiv\text{B}-\text{}$ + $\equiv\dot{\text{S}}\text{i}-\text{Si}\equiv$ to yield $\equiv\text{B}-\dot{\text{S}}\text{i}=\text{}$ are predicted to be 1.0 ± 0.4 and 1.35 ± 0.6 eV, respectively. More details regarding the formation and diffusion of B-related defects will be presented elsewhere. The results suggest that the increase of O vacancy concentration will lead to enhanced B diffusion by rendering diffusion mediators, such as E' and S centers, while B atoms preferentially exist in the form of immobile $\equiv\text{B}-\text{}$ or $\equiv\text{B}-\text{Si}\equiv$. This is consistent with earlier experiments.¹²

Unlike the B case, in an O-deficient region, N atoms prefer to exist in the threefold $\text{N}(\text{Si}\equiv)_3$ configuration [Fig. 2(d)] by consuming O vacancies because of the stronger Si—O bond compared to the Si—N bond. On the other hand, the $\text{O}-\text{N}(\text{Si}\equiv)_2$ configuration [Fig. 2(c)] is often seen in the O-rich environment. The O vacancy scavenger has been evidenced by earlier experiments which demonstrated a reduction in the amount of suboxide Si atoms¹³ as well as the density of E' centers¹⁴ in nitrated SiO₂ films. As illustrated in Fig. 2, we can also expect that O vacancies created by B incorporation will be annihilated by incorporated N atoms. Our cluster model calculations¹⁵ predict an energy gain of 10 eV for the $\equiv\text{Si}-\dot{\text{B}}-\text{}$ + $\text{O}-\text{N}(\text{Si}\equiv)_2 \rightarrow \equiv\text{B}-\text{}$ + $\text{N}(\text{Si}\equiv)_3$ reaction associated with the transfer of an S center (corresponding to 3/2 O vacancies). From the results, we can expect that the N-induced reduction of O vacancy population

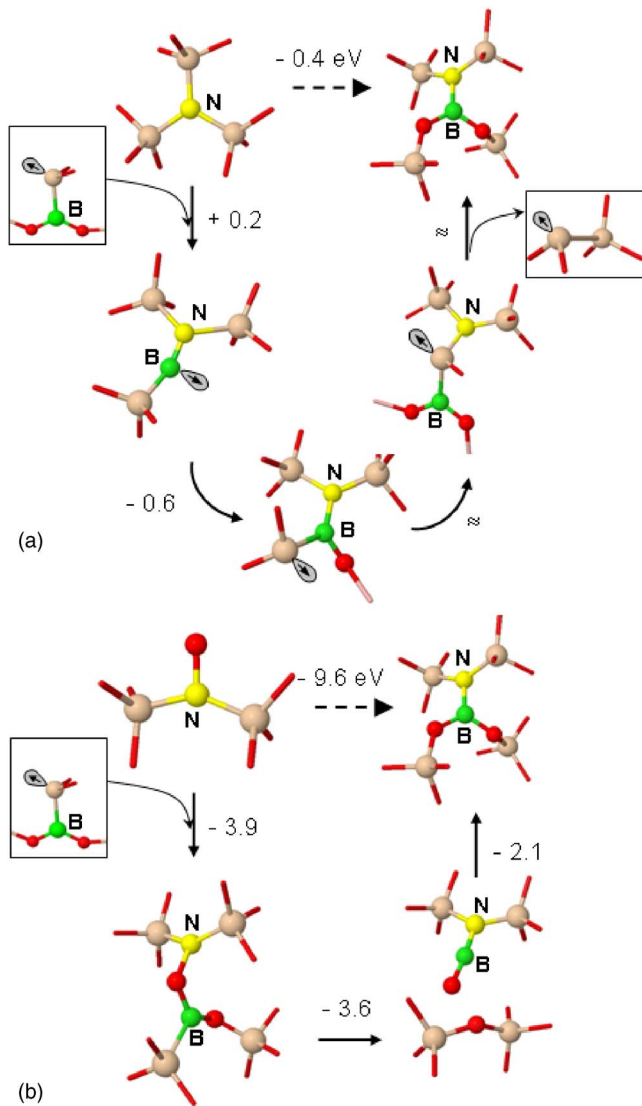


FIG. 3. (Color online) Predicted routes for $2(-\text{O})\text{B}^- + \text{N}(\text{Si}\equiv)_2$ formation by the reaction of mobile $=\text{B}-\dot{\text{S}}\text{i}=\text{Si}\equiv$ with $\text{N}(\text{Si}\equiv)_3$ (a) or $\text{O}-\text{N}(\text{Si}\equiv)_2$ (b). The former and latter reactions are expected to preferentially occur in O-deficient and O-rich regions, respectively. The small dark (red), big gray (pink), and light (green) balls indicate O, Si, and B atoms, respectively. The locations of unpaired electrons are also indicated.

will be largely responsible for B diffusion retardation in the absence of direct B—N bonding interaction.

Next, we examined the direct bonding interaction of B with N. Among various configurations, we find the $2(-\text{O})\text{B}-\text{N}(\text{Si}\equiv)_2$ complex (see Fig. 3) to be most favorable. The B and N atoms adopt trigonal planar geometries. The B—N bond is likely to have a partial double bond character arising from overlap of the filled orbital on N with the empty orbital on B, i.e., $2(-\text{O})\text{B}-\ddot{\text{N}}(\text{Si}\equiv)_2 \leftrightarrow 2(-\text{O})\text{B}^- + \text{N}(\text{Si}\equiv)_2$. Our cluster model calculations $[\text{B}[\text{O}-\text{Si}(\text{OH})_3]_3 + \text{N}[\text{Si}(\text{OH})_3]_3 \rightarrow 2[(\text{OH})_3\text{Si}-\text{O}]\text{B}-\text{N}[\text{Si}(\text{OH})_3]_2 + 3(\text{OH})-\text{Si}-\text{O}-\text{Si}(\text{OH})_3]$ predict that the $2(-\text{O})\text{B}-\text{N}(\text{Si}\equiv)_2$ formation is favored by about 0.4 eV compared to the case of two separate $\text{N}(\text{Si}\equiv)_3$ and $=\text{B}-\text{Si}\equiv$ states, whereas the energy gains only slightly over the range of 0–0.1 eV in our supercell calculations due to larger strains associated with the B—N complex.

Figure 3 also shows two possible routes leading to $2(-\text{O})\text{B}^- + \text{N}(\text{Si}\equiv)_2$ formation. Firstly, as illustrated in Fig. 3(a), in a Si-rich region the mobile $=\text{B}-\dot{\text{S}}\text{i}=\text{Si}\equiv$ defect may react with the most prevailing $\text{N}(\text{Si}\equiv)_3$ species to form the B—N complex with an S center. Secondly, in the O-rich environment, the interaction of $=\text{B}-\dot{\text{S}}\text{i}=\text{Si}\equiv$ with $\text{O}-\text{N}(\text{Si}\equiv)_2$ may result in the B—N complex with no creation of additional defects [Fig. 3(b)]. Both reactions are exothermic, releasing 0.4 and 9.2 eV, respectively. While we admit that there would be other routes with various intermediate states, the results at least demonstrate the possibility of stable B—N complex formation upon introduction of B and N atoms together into *a*- SiO_2 .

By capturing a mobile S center, $2(-\text{O})\text{B}-\text{N}(\text{Si}\equiv)_2$ may dissociate into $\text{N}(\text{Si}\equiv)_3$ and $=\text{B}-\dot{\text{S}}\text{i}=\text{Si}\equiv$, i.e., $2(-\text{O})\text{B}-\text{N}(\text{Si}\equiv)_2 + =\dot{\text{S}}-\text{Si}\equiv \rightarrow \text{N}(\text{Si}\equiv)_3 + =\text{B}-\dot{\text{S}}\text{i}=\text{Si}\equiv$ [via the reverse path of B—N complex formation, as seen in Fig. 3(a)]. The reaction appears endothermic by as much as 0.1–0.4 eV depending on the local strain environment, as opposed to no noticeable energy change in $=\text{B}- + =\dot{\text{S}}-\text{Si}\equiv \rightarrow =\text{B}-\dot{\text{S}}\text{i}=\text{Si}\equiv$. Assuming the $=\text{B}-\dot{\text{S}}\text{i}=\text{Si}\equiv$ complex is mobile, this implies that the direct B—N bonding interaction may lead to an increase in the overall activation energy of B diffusion, albeit insignificantly. This is consistent with earlier experiments which also showed an increase in the diffusion activation energy, in the range of a few tens of an eV.¹⁶

We acknowledge National Science Foundation (CAREER-CTS-0449373 and ECS-0304026), Robert A. Welch Foundation (F-1535), and Tokyo Electron, Ltd. for their financial support. We would also like to thank the Texas Advanced Computing Center for use of their computing resources.

- ¹W. B. Fowler and A. H. Edwards, *J. Non-Cryst. Solids* **222**, 33 (1997).
- ²R. B. Fair, *J. Electrochem. Soc.* **144**, 708 (1997).
- ³K. C. Snyder and W. B. Fowler, *Bull. Am. Phys. Soc.* **39**, 539 (1994).
- ⁴M. Uematsu, H. Kageshima, and K. Shiraishi, *Jpn. J. Appl. Phys., Part 1* **44**, 7756 (2005).
- ⁵Z. J. Ma, J. C. Chen, Z. H. Liu, J. T. Krick, Y. C. Cheng, C. Hu, and P. K. Ko, *IEEE Electron Device Lett.* **15**, 109 (1994).
- ⁶D. Yu, G. S. Hwang, T. A. Kirichenko, and S. K. Banerjee, *Phys. Rev. B* **72**, 205204 (2005), and the references cited therein.
- ⁷T. Kirichenko, D. Yu, S. Banerjee, and G. S. Hwang, *Phys. Rev. B* **72**, 35345 (2005).
- ⁸C.-L. Kuo and G. S. Hwang, *Phys. Rev. Lett.* **97**, 66101 (2006).
- ⁹C.-L. Kuo, S. Lee, and G. S. Hwang, *Phys. Rev. Lett.* **100**, 76104 (2008).
- ¹⁰J. P. Perdew and Y. Wang, *Phys. Rev. B* **45**, 13244 (1992).
- ¹¹G. Kresse and J. Furthmüller, *VASP: The Guide* (Vienna University of Technology, Vienna, Austria, 2001).
- ¹²M. Uematsu, H. Kageshima, Y. Takahashi, S. Fukatsu, K. M. Itoh, and K. Shiraishi, *Appl. Phys. Lett.* **85**, 221 (2004).
- ¹³Z. H. Lu, S. P. Tay, R. Cao, and P. Pianetta, *Appl. Phys. Lett.* **67**, 2836 (1995).
- ¹⁴J. T. Yount, P. M. Lenahan, and G. J. Dunn, *IEEE Trans. Nucl. Sci.* **39**, 2211 (1992).
- ¹⁵(1) $(\text{HO})_3\text{Si}-\text{B}-\text{O}-\text{Si}(\text{OH})_3 + 2(\text{HO})_3\text{Si}-\text{O}-\text{Si}(\text{OH})_3 \rightarrow (\text{HO})_2\text{B}-\text{O}-\text{Si}(\text{OH})_3 + [(\text{HO})_3\text{Si}]_2(\text{HO})\text{Si}-\text{Si}(\text{OH})_3 + 1/2(\text{HO})_3\text{Si}-\text{Si}(\text{OH})_3$, which involves the conversion of B into B_2O_3 and $3/2$ OV. (2) $\text{O}-\text{N}-[\text{Si}(\text{OH})_3]_2 + 3/2(\text{HO})_3\text{Si}-\text{Si}(\text{OH})_3 \rightarrow \text{N}[\text{Si}(\text{OH})_3]_3 + (\text{HO})_3\text{Si}-\text{O}-\text{Si}(\text{OH})_3$. The energy gains for (1) and (2) are 2.3 and 7.7 eV, respectively, yielding the total energy gain of 10 eV.
- ¹⁶T. Aoyama, K. Suzuki, H. Tashiro, Y. Toda, T. Yamazaki, K. Takasaki, and T. Ito, *J. Appl. Phys.* **77**, 417 (1995).